Acoustic backscattering at low grazing angles from the ocean bottom. Part I. Bottom backscattering strength

H. Boehme, N. P. Chotiros, L. D. Rolleigh, S. P. Pitt, A. L. Garcia, T. G. Goldsberry, and R. A. Lamb

Applied Research Laboratories, The University of Texas at Austin, P. O. Box 8029, Austin, Texas 78713-8029

(Received 21 June 1984; accepted for publication 2 October 1984)

Acoustic backscattering measurements on a sand bottom were made at grazing angles in the range of about 2°–10° in water depth of approximately 15.5 m near San Diego, California (reported by T. G. Goldsberry, S. P. Pitt, and R. A. Lamb, 104th Meeting of the Acoustical Society of America, Orlando, FL, 8–12 November 1982). Data from these measurements have been analyzed to determine the mean value and standard deviation of the bottom backscattering strength per square meter as a function of grazing angle, insonified area, transmit signal type, and frequency. A curved ray path proportional model and measured sound speed profiles were used to determine grazing angle versus time. The mean value followed Lambert's law for the range of grazing angles measured and for all frequencies used. No significant differences in mean value were observed when the insonified area and transmit signal type were varied. The observed frequency dependence of the bottom backscattering strength per square meter falls in the range from $f^{1.0}$ to $f^{1.5}$ for this relatively flat, sandy bottom.

PACS numbers: 43.30.Bp, 43.30.Gv, 92.10.Vz, 91.50.Ey

INTRODUCTION

Acoustic bottom backscattering measurements were made in May 1982 about 1 mi offshore from Mission Beach, California. The measurements were made using transducers mounted on a tripod assembly about 4 m tall that rested on the bottom. The horizontal and vertical orientation of the transducers were controlled and monitored by test personnel on a nearby oceanographic tower. The acoustic measurements were made over a range of grazing angles of 2°–10° and a range of frequencies of 30–95 kHz. Details of the measurement system as well as the bottom backscattering measurements that were made have been presented previously.[1]

A preliminary objective of the bottom backscattering measurements was to provide data at low grazing angles from which backscattering strength values and reverberation statistics could be extracted. Several comprehensive reviews have been published which include bottom backscattering strength versus grazing angle in the 20–100 kHz frequency range.[2-4] The most notable of these, by McKinney and Anderson[2] and by Shultz,[3] are almost 20 years old; only a few measurements at grazing angles below 10° are included. The more recent review by Bunchuk and Zhitkovskii[4] includes information at low grazing angles. These reviews generally agree that bottom backscattering can be broadly categorized according to bottom composition, such as mud or silt, sand, and rock or gravel. However, relatively large variations within each general bottom type are common, with little or no correlation of bottom backscattering strength with mean particle size within each of the categories. For grazing angles above about 2°, backscattering was reported to increase with grazing angle according to $\sin^k \theta$, where θ is the grazing angle and k is a number between 1 and 2. For sand sediments, backscattering was found by McKinney and Anderson[2] to increase with frequency while Bunchuk and Zhitkovskii[4] concluded that backscattering was independent of frequency, or at most only slightly dependent on frequency, for all bottom types.

The acoustic measurements made in shallow water near San Diego were specifically planned to provide bottom backscattering data for low grazing angles over a relatively wide range of frequencies. The transmitted pulse waveforms were either cw (pulse lengths of 0.25–25 ms) or linear FM (1–25 ms pulses with 1–4 kHz bandwidths) and were generally transmitted on alternate pings until approximately 75 pings of each pulse type had been transmitted.

Physical oceanographic measurements were made by Naval Ocean Research and Development Activity (NORDA) during the same period of time that acoustic measurements were made. A report on the sediment geoacoustic properties has been written and distributed.[5]

I. DATA ANALYSIS DESCRIPTION

The acoustic measurement data were recorded on analog magnetic tape records, converted to digital data records by use of general purpose analog-to-digital (A/D) equipment, and processed by use of analysis software written for a general purpose computer (CDC CYBER 171). The digital data record format was such that each transmitted pulse and subsequent reverberation period was identified by pulse type, frequency, time, and number of sequential samples composing the digital data record. An envelope was generated for each ping and was then smoothed by time averaging with a moving time window equal in length to the pulse duration.

A number of sequential ping cycles (usually 30 to 50) using the same pulse waveform were assembled to form an ensemble. Statistical tests were then performed in order to assure that the assembled envelope records constituted a val-

 0001-4966/85/030962-13$00.80 © 1985 Acoustical Society of America

id ensemble. An existing ray tracing computer program was used to relate time after initiation of the pulse transmission to path length, horizontal range, and grazing angle. A horizontally stratified water column based upon a measured sound speed profile was assumed within the ray tracing computations. A mean backscattering strength and a standard deviation from the mean were calculated for the ensemble of envelope data records.

The mean backscattering strength BS, in dB/m^2, was calculated according to the following equation:

$$\mathrm{BS} = RL - SL - 2TL - 10\log[A_s D_{pu}^2(\theta_1) D_{hv}^2(\theta_2)] , \quad (1)$$

where

RL = equivalent returned signal level on the hydrophone MRA in dB *re*:1 μPa.

SL = acoustic projector on-axis source level in dB *re*:1 μPa at 1 m,

$2TL$ = two-way propagation loss, in dB,

A_s = effective insonified area, in m^2,

$D_{pu}^2(\theta_1)$ = vertical directivity function of the projector intensity as a function of θ_1, the angular separation between the maximum response axis (MRA) and the launch angle of the outward ray path, and

$D_{hv}^2(\theta_2)$ = vertical directivity function of the hydrophone as a function of θ_2, the angular separation between the receive MRA and the termination angle of the return ray path.

Since the returned signal level RL associated with each path length, range, or grazing angle varies from ping to ping, the power-averaged value was used for backscattering strength computations. Thus, the ensemble average of the square of the envelope was computed and halved, and then the square root taken to obtain RL since narrow-band signals were assumed.

In the assumed horizontally stratified medium with nonuniform sound speed versus depth, the spreading loss portion L_S of the propagation loss TL was computed by tracing two rays at slightly different vertical launch angles and determining their separation at the points of bottom contact. In this manner, a correction factor C_S was determined which arises due to divergence or convergence of the sound rays. The correction factor C_S was the ratio of the actual area insonified perpendicular to the two adjacent rays to the ideal insonified area assuming spherical spreading at the same path length l and within the same launch angle interval θ_{ld}. Then, C_S was given by

$$C_S = r\, r_d \sin\theta_g / l^2 \theta_{ld} \cos\theta_l , \quad (2)$$

where

r = average horizontal range to the points of bottom contact of the two adjacent rays,

r_d = difference in horizontal range of the two points,

θ_g = average grazing angle of the two rays with the bottom,

l = path length along an ideal straight line ray path,

θ_{ld} = difference in adjacent ray launch angles, and

θ_l = average launch angle of two rays with respect to the horizontal.

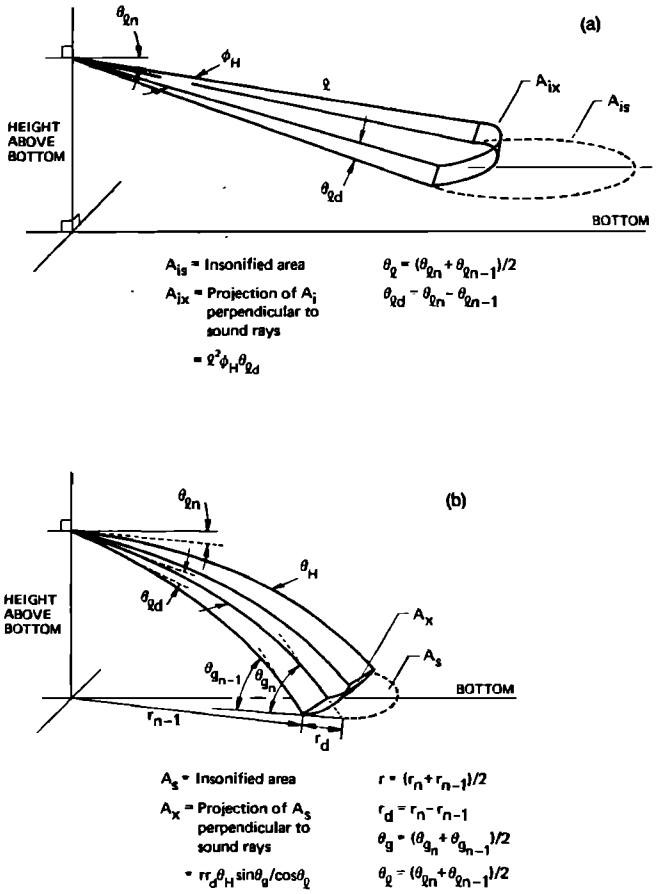

FIG. 1. Spreading of rays at path length l, launch angle θ_l. (a) Ideal case, (b) practical case.

The one-way spreading loss L_S in dB was expressed as the ideal spherical spreading loss with the correction factor C_S as follows:

$$L_S = -20\log l - 10\log C_S . \quad (3)$$

Large numerical values of C_S are indicative of shadow zones while small values are indicative of focusing.

The absorption loss part of the propagation loss was calculated by combining the ray-traced path length and the absorption coefficient (in dB/m), where the absorption coefficient was determined from the Shulkin and Marsh[6] equation. The total one-way propagation loss including absorption loss was expressed as

$$TL = -20\log l - 10\log C_S - \alpha l . \quad (4)$$

Calculation of the effective insonified area also made use of the ray-tracing computer program. Figure 1 shows sketches of (a) the geometry for ideal (isovelocity) conditions and (b) the geometry used when the medium is assumed to be horizontally stratified with depth-dependent sound speed. When curved ray paths and low grazing angles are appropriate, the expression used for the insonified area is as follows:

$$A_s = (r\phi_H)[(C_b \tau/2)\sec\theta_g] , \quad (5)$$

where r is the horizontal range, ϕ_H is the effective horizontal beamwidth of the projector and hydrophone array, c_b is the sound speed just above the bottom, τ is the pulse length, and θ_g is the grazing angle.

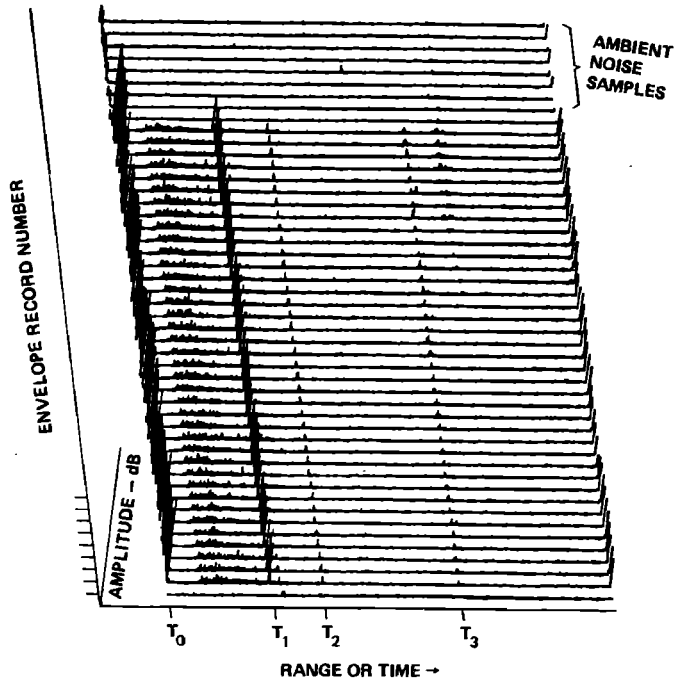

FIG. 2. Three-dimensional plot of an ensemble of sequential envelope records when propagation conditions were relatively stable. Transmitted pulse was 0.25-ms cw and events on the range/time axis are T_0 = transmit, T_1 = acoustic target at 70-m range, T_2 = acoustic target at 110-m range, and T_3 = acoustic target at 210-m range.

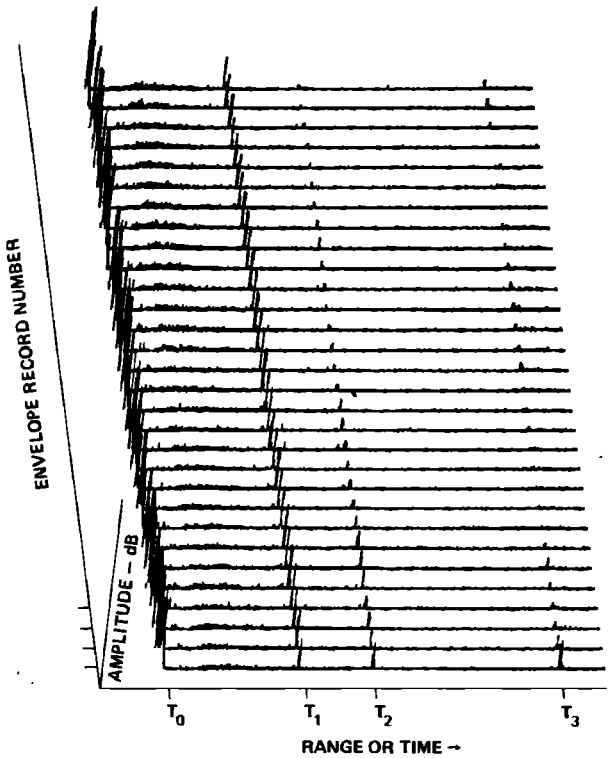

FIG. 3. Three-dimensional plot of an ensemble of sequential envelope records when propagation conditions were unstable. Transmitted pulse was 0.25-ms cw and events on the range/time axis are the same as those in Fig. 2.

The effective horizontal beamwidth ϕ_H of the projector and hydrophone array is approximated in terms of the -3 dB horizontal beamwidths of the hydrophone array ϕ_h and the projector ϕ_p according to the following expression:

$$\phi_H \approx 1.065(\phi_h^{-2} + \phi_p^{-2})^{-1/2}, \quad \text{in radians}, \tag{6}$$

where ϕ_h and ϕ_p are also expressed in radians and the numerical factor arises from an assumption that the mainlobes of the actual hydrophone and projector horizontal directivity functions are approximated by Gaussian functions.

The expression given in Eq. (5) for the insonified area assumes that grazing angle is a constant over the instantaneous insonified area; this is an acceptable approximation only if the sound speed profile does not result in focusing or shadow zones within the acoustic measurement region of interest. Inaccuracies in grazing angle estimation are propagated to estimates of the insonified area.

The acoustic projector on-axis source level (SL) versus transmit electrical current was determined by acoustic calibration at the Lake Travis Test Station (LTTS) calibration facility prior to making the acoustic backscattering measurements. The transmit current was monitored during the measurements and recorded on data log sheets.

The projector and hydrophone vertical directivity functions were also measured and recorded on data log sheets at LTTS. The vertical directivity functions were digitized and stored in a digital calibration data file which could be accessed as needed during the analysis of measurement data.

II. DATA ANALYSIS RESULTS

The acoustic data were analyzed to determine the behavior of bottom backscattering strength as a function of grazing angle, effective horizontal beamwidth, transmit signal type, frequency, and bottom type. Since backscattering strength was calculated by averaging over an ensemble of envelope records, an attempt was made to select data representative of the characteristic being investigated over a time interval during which propagation conditions remained relatively stable. In addition to statistical tests used to indicate valid ensembles, three-dimensional plots were generated allowing visual indications of the stability of the medium. Figure 2 is an example of such a plot, showing the envelope records of sequential pings of a particular pulse type when propagation conditions were relatively stable. Figure 3 is a similar plot showing unstable propagation conditions as evidenced by the variation in amplitudes for adjacent ping cycles. The time between pings in both figures was 1 s.

A. Bottom backscattering strength versus grazing angle

Initial estimates of backscattering strength were carried out using theoretical estimates of the transducer beam patterns and assuming a constant sound speed versus depth profile. The results obtained were reliable only for ranges less than about 25 m, which corresponded to grazing angles of 10° or more. For lower grazing angles and correspondingly longer ranges, the sound speed profile was found to have a significant influence on the results. Examples are shown in Figs. 4 and 5, in which the estimated backscattering strengths as a function of grazing angle are presented. Figure 4 represents estimates based on a constant sound speed versus depth assumption, while Fig. 5 represents estimates based on a measured sound speed profile in conjunction with

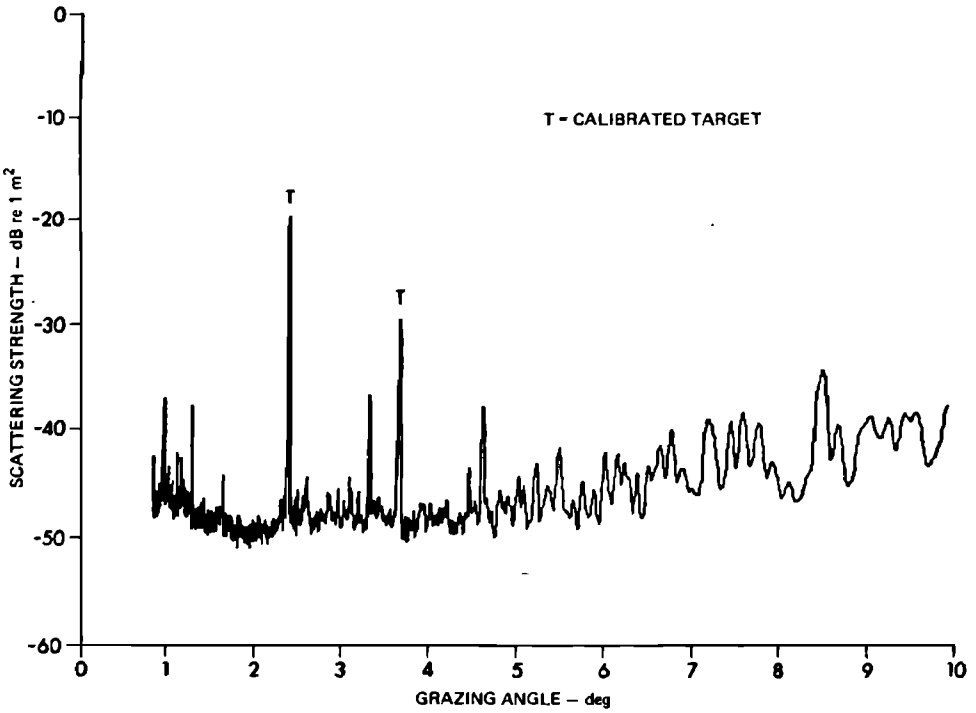

FIG. 4. An example of backscattering strength estimates as a function of grazing angle where a constant sound speed versus depth was assumed. Frequency = 30 kHz.

a ray tracing computer program. The results shown in Fig. 4 indicate that grazing angles of 10°–1° were being measured, while those of Fig. 5 indicate that, in reality, the downward refraction caused by the sound speed profile limited the grazing angles to values above about 2.5°.

Ray tracing was also used to determine the range, propagation delay, and grazing angle of a few key ray paths, such as the rays at the — 3 dB points of the vertical beam patterns, and the rays from the center of the mainlobe and the sidelobes. The information was provided in the form of a printout which accompanies the graphical result. Some of this information is illustrated in Fig. 5. The information is particularly useful for checking anomalous features in the bottom backscattering strength estimates. Other propagation anomalies, including focusing and shadow zones, are also printed out as warning messages as they are detected.

In order to determine the sensitivity of grazing angle to input sound speed profile, a particular block of data was processed using sound speed profiles measured on two successive days (5–6 May) as inputs. The reverberation data used were recorded approximately 2 1/2 h after the sound speed profile was measured on 5 May. A comparison of backscattering strength versus grazing angle is shown in Fig. 6 for input sound speed profiles measured on 5–6 May. Since

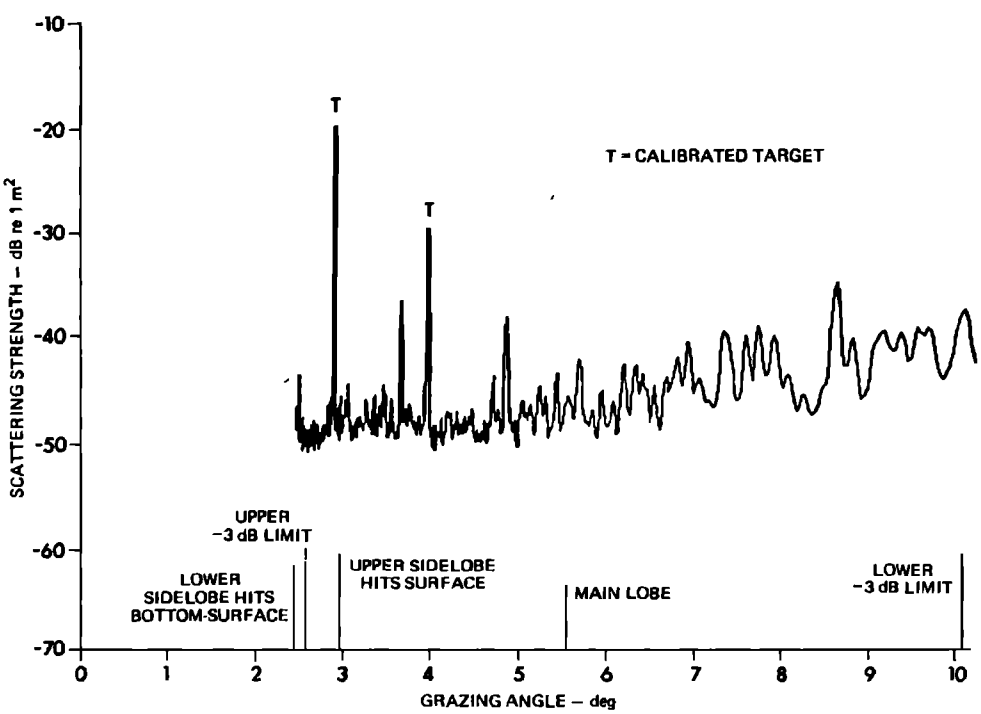

FIG. 5. An example of backscattering strength estimates as a function of grazing angle, with ray tracing and a measured sound speed profile. Frequency = 30 kHz.

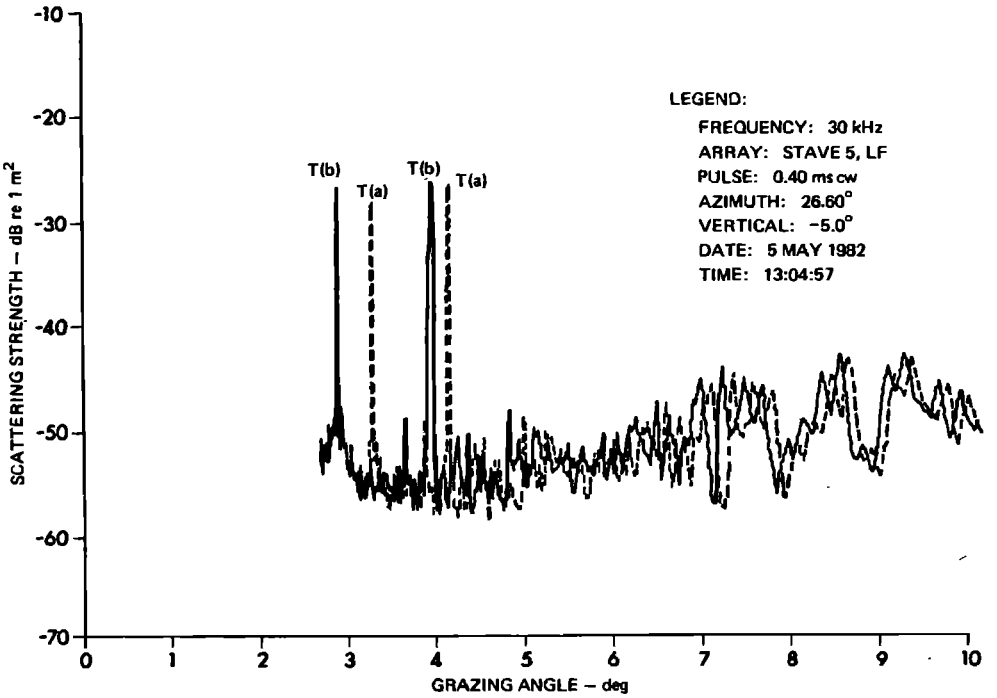

FIG. 6. An example of backscattering strength versus grazing angle estimated based upon the same data set and two different sound speed profiles. Curve (a) corresponds to estimates made with an input sound speed profile measured approximately 2 h before the acoustic measurement; curve (b) corresponds to estimates made with a sound speed profile measured approximately one day later than the acoustic measurements.

the same reverberation data were used for both plots in Fig. 6, the two input sound speed profiles used cause differences of less than 0.5° in grazing angles for corresponding bottom features (and calibrated acoustic targets, as indicated).

The bottom backscattering measurements were intended to provide information at grazing angles below about 15°. The low grazing angle limit, corresponding to longer ranges, was observed to depend upon the propagation conditions existing at the time the particular backscattering measurements were made. In particular, the sound speed profile was such that downward refraction prevented meaningful measurements below about 2°, since energy backscattered from the bottom became contaminated by energy backscattered from the sea surface at the longer ranges.

The surface reverberation contribution resulted from a direct surface path as well as a bottom bounce to surface path with the same two-way travel time as the direct bottom path for bottom backscattering at longer ranges. The sketch in Fig. 7 is helpful in describing the relationship between bottom and surface backscattering. At shorter ranges the bottom-surface and direct surface paths (solid lines) with the same two-way travel time as the direct bottom path are associated with the sidelobe region of the projector and receiver vertical beam patterns. The surface reverberation levels are not sufficient to seriously affect the bottom reverberation level. However, at longer ranges, the bottom surface and direct surface paths (dashed lines) are associated with beam pattern regions that are migrating toward the beam MRA. The direct bottom path, conversely, is associated with beam pattern regions that are migrating away from the beam MRA as the range increases. At some range, depending upon existing propagation conditions and sea surface conditions, the surface reverberation level can become comparable with or greater than the bottom reverberation level. This condition imposes a lower grazing angle limit on the analyses of bottom backscattering strength.

To confirm that the background noise level associated with low grazing angles was indeed contaminated by surface reverberation, the background levels were first compared with measured ambient noise levels. The observed background levels were significantly above ambient noise levels and were observed to depend upon transmitted signal pulse length. The observed background level at the longer ranges was also found to be correlated with wind speed. On occa-

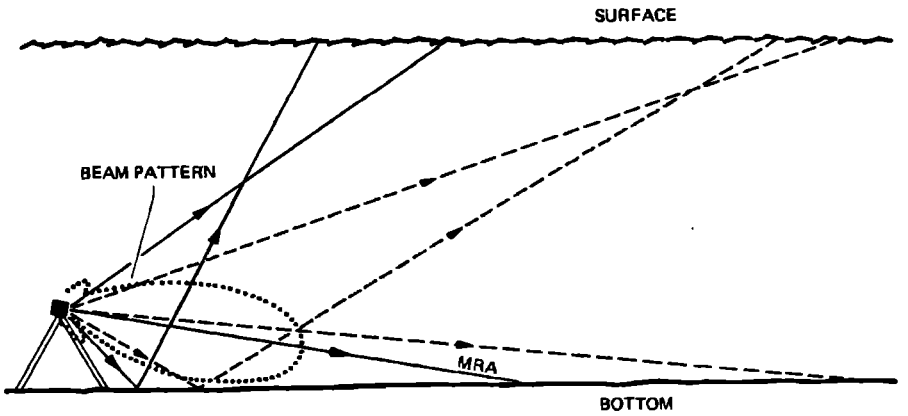

FIG. 7. Contamination at longer ranges of bottom backscattering measurements by surface backscattering.

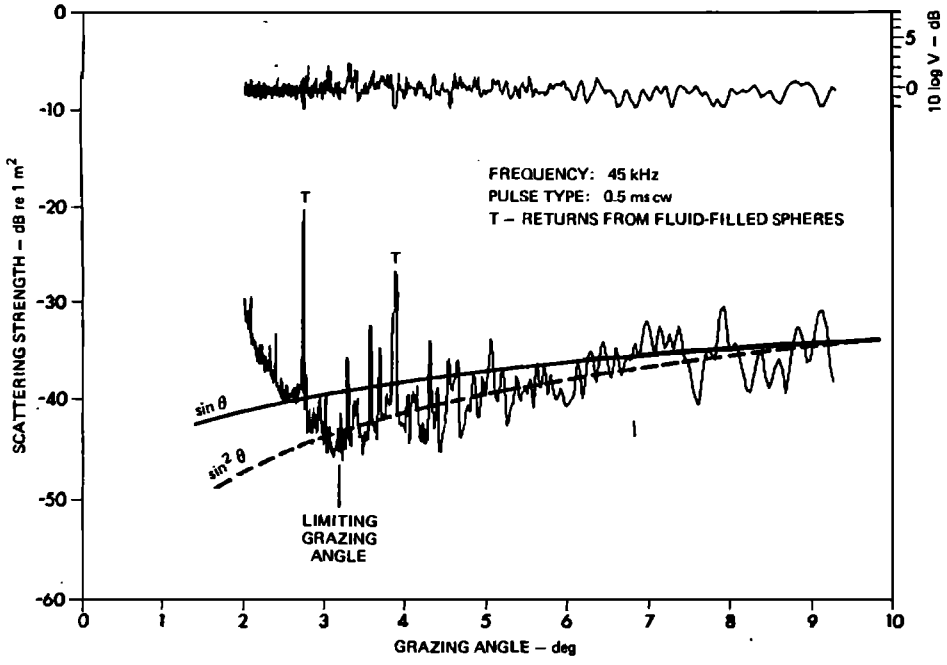

FIG. 8. An example of observed bottom backscattering strength which has significant contamination by sea surface backscattering below the indicated grazing angle.

sions when the sea surface was very rough, the trend of the estimated backscattering strength decreased with decreasing angle from about 10° down to 3° or 4°; this trend would then abruptly change and increase with decreasing grazing angle.

An example of observed bottom backscattering strength versus grazing angle at 45 kHz is shown in Fig. 8 for which contamination by surface reverberation becomes significant at about 3° grazing angle. Thus, the useful range of bottom backscattering strength information lies between about 3° and 9.5°. Within this region of grazing angles the trend (dashed line) of the bottom backscattering strength follows that of 10 log ($\sin^2 \theta$), where θ is the grazing angle. This Lambert's rule behavior, discussed by Urick,[7] is not uncommon for observed backscattering at low grazing angles for bottom conditions where the roughness scale is the same order as the acoustic wavelength. For comparison, a solid line representing a trend of 10 log ($\sin \theta$) is also shown in Fig. 8.

A measure of the variation of bottom backscattering strength versus grazing angle was calculated for each ensemble of envelope records. The measure used was the coefficient of variation (the standard deviation from the mean divided by the mean value) at each grazing angle. An example of this measure is shown in Fig. 8 where the quantity 10 log V versus grazing angle has been plotted, where V is the coefficient of variation.

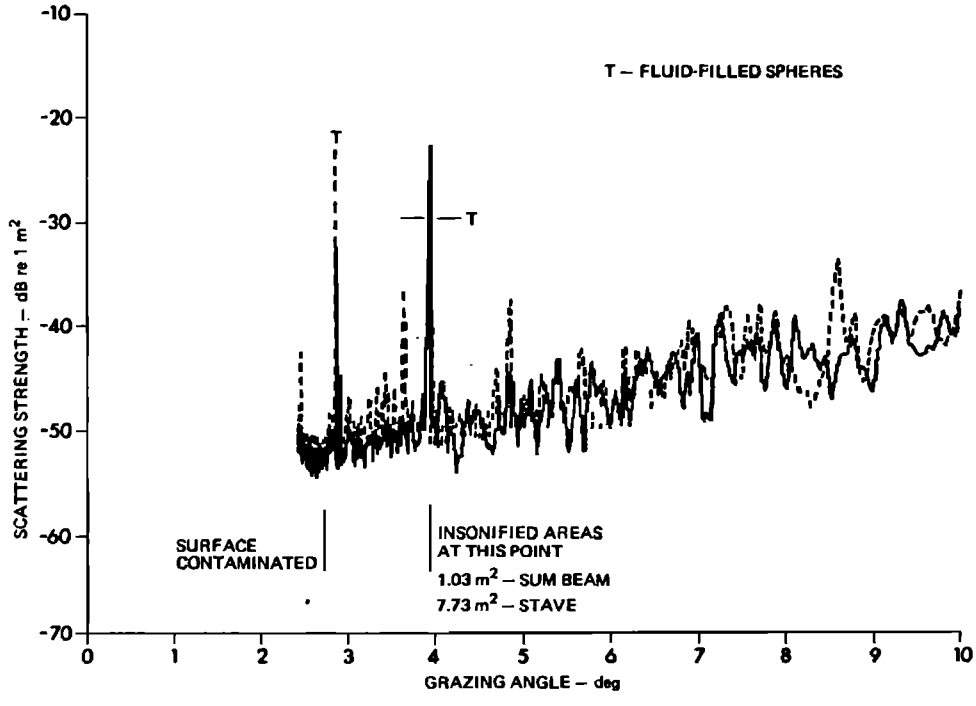

FIG. 9. Comparison of backscattering strength estimates at 30 kHz using a combined azimuthal beamwidth of (a) 21.1° (solid line) and (b) 2.8° (dashed line). In both cases a cw pulse of 0.4 ms was used.

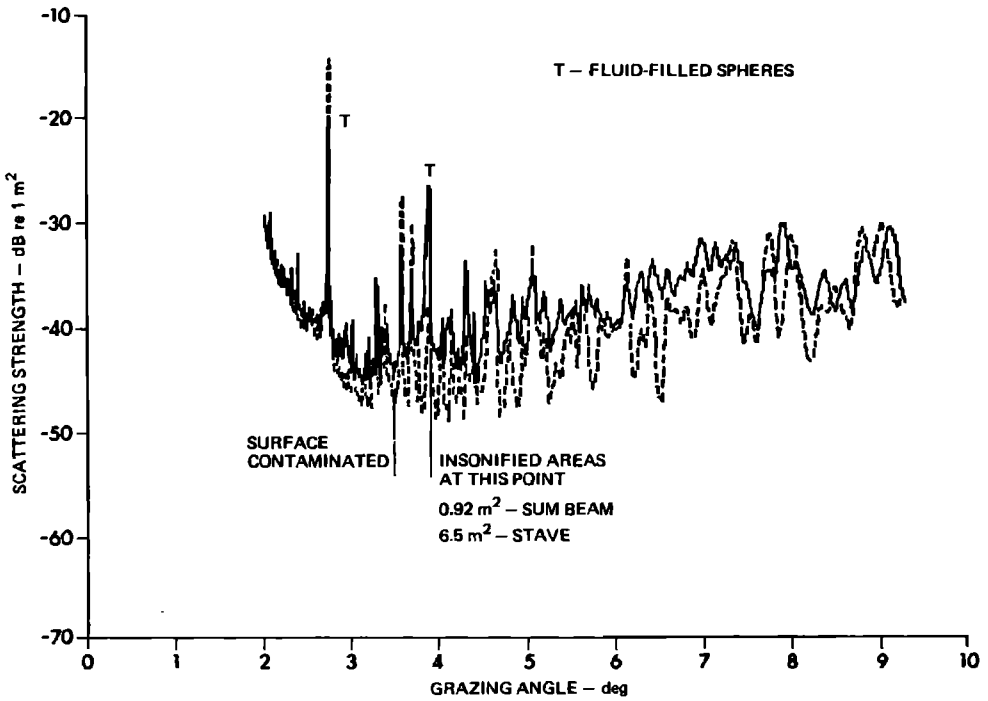

FIG. 10. Comparison of backscattering strength estimates at 45 kHz using a combined azimuthal beamwidth of (a) 14.2° (solid line) and (b) 2.0° (dashed line). In both cases a 0.5-ms cw pulse was used.

B. Beamwidth dependence of bottom backscattering strength

Both sum beam and individual receiving array stave outputs were recorded during the experiments. Figures 9–13 show comparisons of estimated backscattering strength for the beamwidths of the sum beams and staves of the receiving arrays for frequencies of 30–95 kHz. The corresponding insonified areas are indicated at a common range point of 70 m on all the figures. For the examples shown, and for other pulse types analyzed, there was no observed dependence of mean bottom backscattering strength on beamwidth. (Minor differences noted in the reverberation statistics are given in an accompanying paper.) In all cases the variation of the curves from the general trend with grazing angle was noticeably less for the larger beamwidths associated with the staves than for the beamwidths associated with the sum beams. The general trend with grazing angle for both stave and sum beam results at all frequencies was observed to follow Lambert's rule, as shown in Fig. 8.

C. Pulse type dependence

The average bottom backscattering strength versus grazing angle exhibited no dependence upon pulse type or pulse length. Examples of results obtained using the sum

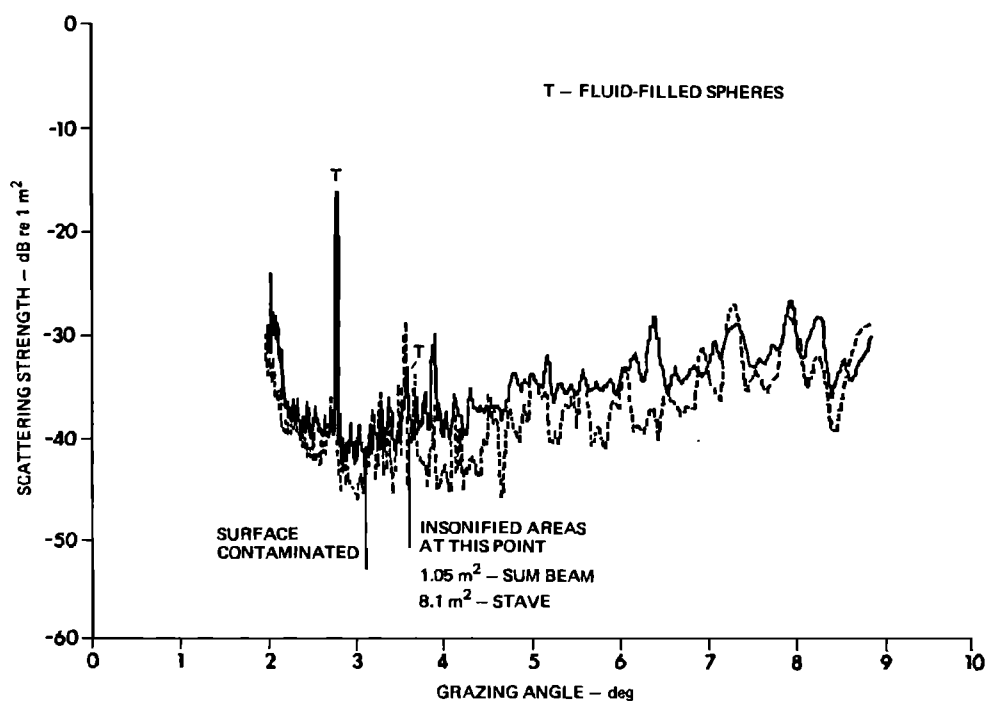

FIG. 11. Comparison of backscattering strength estimates at 60 kHz using a combined azimuthal beamwidth of (a) 17.7° (solid line) and (b) 2.3° (dashed line). In both cases a 0.5-ms cw pulse was used.

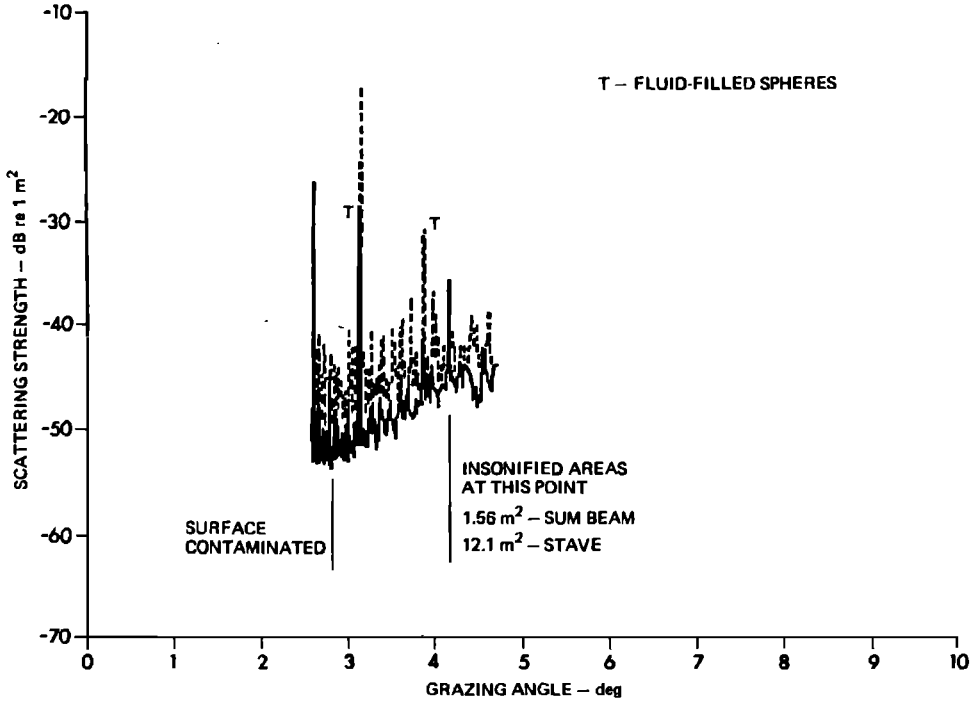

FIG. 12. Comparison of backscattering strength estimates at 80 kHz using a combined azimuthal beamwidth of (a) 13.2° (solid line) and (b) 1.7° (dashed line). In both cases a 0.5-ms cw pulse was used.

beam outputs are shown in Figs. 14–18 for frequencies of 30–95 kHz. In each case, it can be seen that the bottom backscattering strength associated with each pulse type tended to vary randomly about the same mean value. The results for the FM slide pulse types, with a time-bandwidth product greater than unity, were smoother; all the data have been smoothed by averaging over the pulse length.

D. Frequency dependence

The bottom backscattering strength as a function of grazing angle was found to fit Lambert's rule fairly well for all frequencies and pulse types used. Therefore the backscattering strength B_s may be expressed as

$$B_s = 10 \log \mu + 10 \log(\sin^2 \theta), \tag{7}$$

where θ = grazing angle and $10 \log \mu$ = backscattering strength in dB at normal incidence if Lambert's rule were valid at normal incidence.

A $\sin^2 \theta$ function was fitted to each backscattering strength versus grazing angle curve and the value of $10 \log \mu$ was estimated. The quantity $10 \log \mu$ was then plotted as a function of frequency; the results are shown in Fig. 19.

Within the particular bottom region for which Fig. 19 applies (fine sand) and over the frequency range considered here, an increase in bottom backscattering strength with frequency was observed. Due to the scatter in the data points, a frequency dependence of $10 \log f^n$, where $1 < n < 1.5$, can be

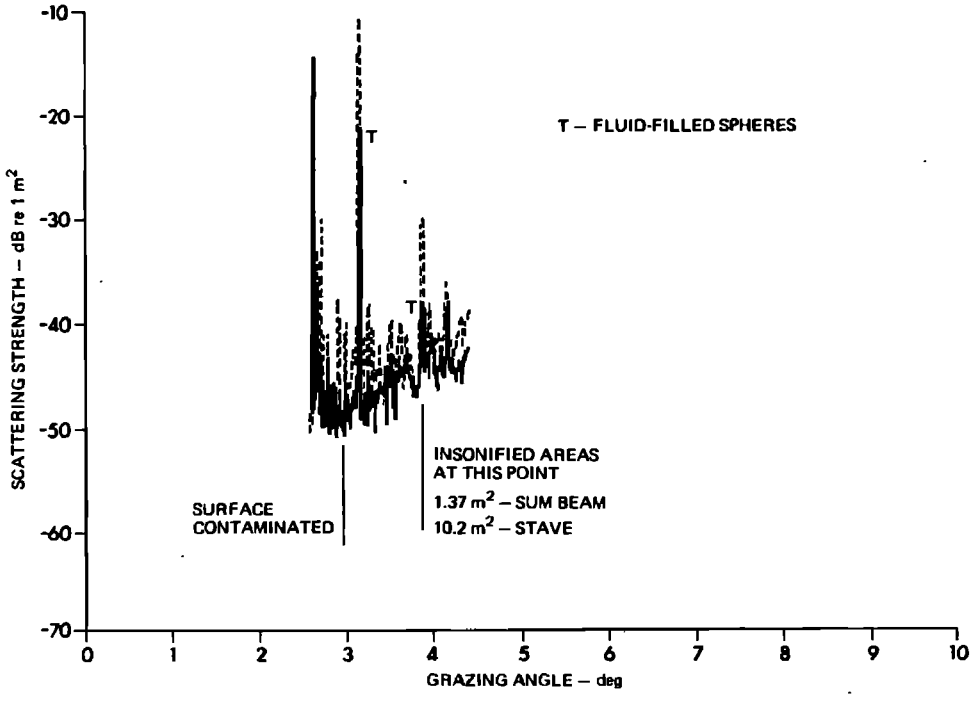

FIG. 13. Comparison of backscattering strength estimates at 95 kHz using a combined azimuthal beamwidth of (a) 11.1° (solid line) and (b) 1.5° (dashed line). In both cases a 0.5-ms cw pulse was used.

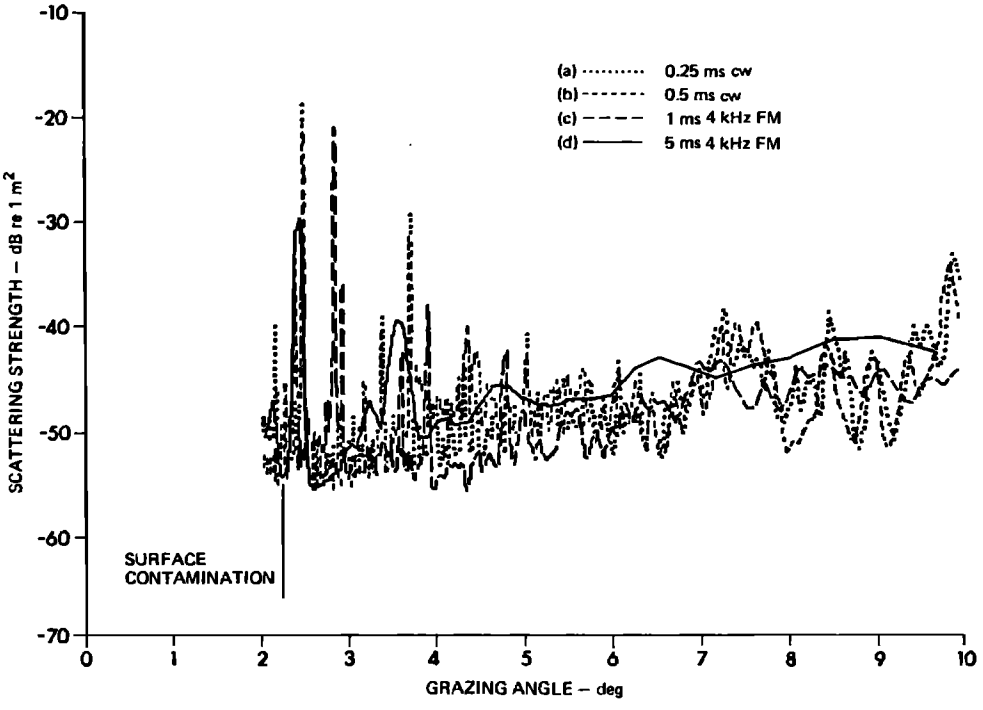

FIG. 14. Comparison of backscattering strength at 30 kHz using (a) 0.25-ms cw, (b) 0.5-ms cw, (c) 1-ms, 4-kHz FM, and (d) 5-ms, 4-kHz FM pulse types.

inferred. This frequency dependence is consistent with that reported by McKinney and Anderson (Ref. 2) of approximately 10 $\log f^{1.6}$ for field measurements in sand bottom regions. Two points are also shown in Fig. 19 at 100 kHz that were estimated from data below 10° grazing angle[2] for sand of about the same particle size as reported in Ref. 5. These points compare very well with data plotted at 95 kHz from the current measurements.

Data reported by Wong and Chesterman[8] for measurements at low grazing angle in a silty sand region at 48 kHz are 15–20 dB higher than data plotted at 45 kHz from the current measurements. The observed values of 10 $\log \mu$ for 30 and 45 kHz shown in Fig. 19 are also substantially lower than results reported by Crisp *et al.*[9] at 30 and 48 kHz for two sites in the Puget Sound. No particular frequency dependence was observed in the results from the Puget Sound measurements (at 20° grazing angle[9]).

Bottom backscattering measurements were reported[2] for a water/sand boundary where the sand had been carefully smoothed. Values of 10 $\log \mu$ for grazing angles from about 3°–10° and frequencies of 57 and 90 kHz were deduced from Ref. 2, and are shown in Fig. 19. A straight line through these two points indicates a frequency dependence of 10 $\log f^{1.8}$, in good agreement with the current measurements. The level of the backscattering from smooth sand is 10–12 dB below that observed in the current measurements. The high-

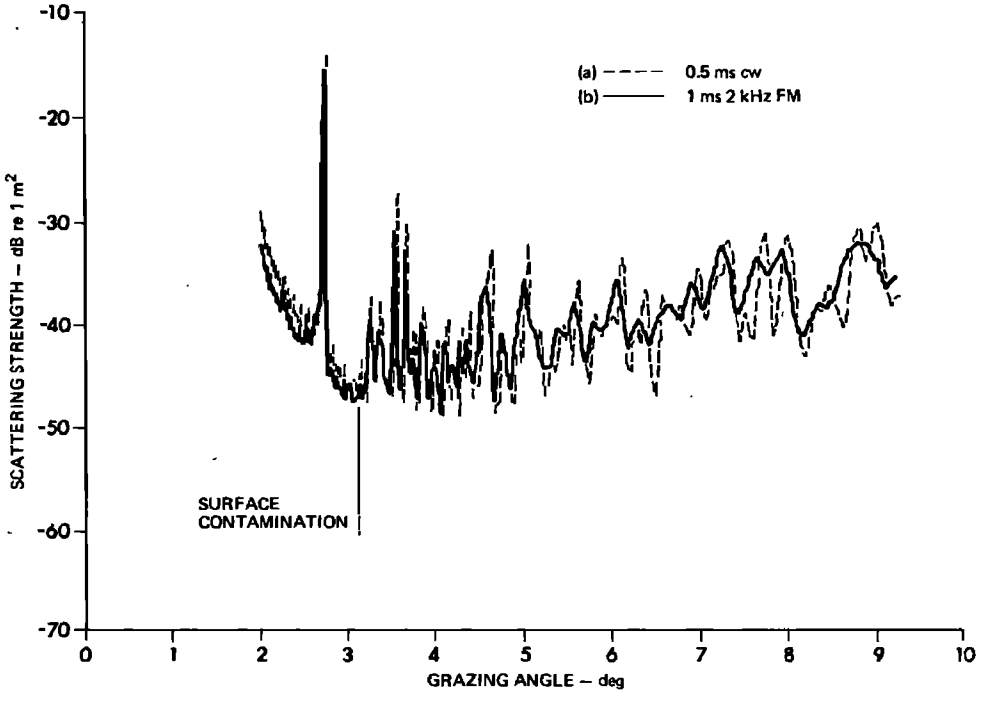

FIG. 15. Comparison of backscattering strength at 45 kHz using (a) 0.5-ms cw and (b) 1-ms, 2-kHz FM pulse types.

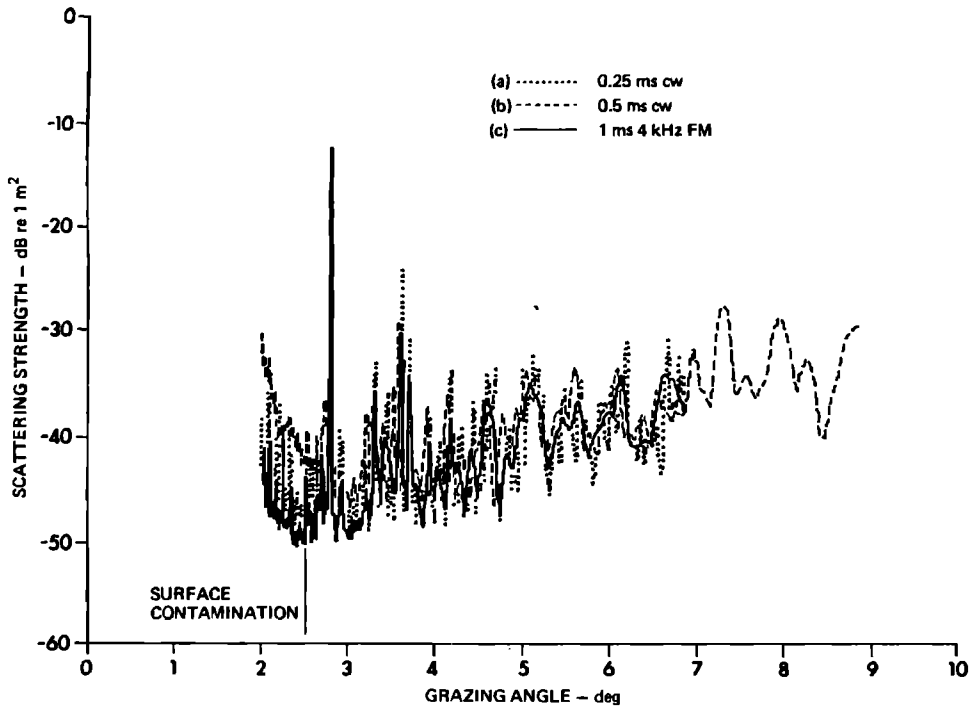

FIG. 16. Comparison of backscattering strength at 60 kHz using (a) 0.25-ms cw, (b) 0.5-ms cw, and (c) 1-ms, 4-kHz FM pulse types. [Note: Curves (a) and (c) obtained with vertical tilt angle of $-3°$ while curve (b) obtained with vertical tilt angle of $-5°$.]

er values observed in the current measurements are undoubtedly due to the interface relief which was purposely missing in the smooth sand measurements.

E. Azimuth dependence

For the purpose of measuring azimuth dependence, a set of data was taken at 30 kHz in which the sonar beam was slowly scanned over a large sector of the bottom. The bottom may be separated into two regions—fine sand and coarse sand regions—with a discernible boundary between them.[5] The scan data included measurements in both regions. The sonar beam was tilted vertically at a depression angle of 5°. At this depression angle, the bottom reverberation returns started at a range of about 25 m, at a grazing angle of 10°. Unfortunately, due to strong surface activity at the time of the experiment, the bottom backscattering data, beyond a range of about 70 m, were severely contaminated by surface backscatter; therefore only data corresponding to ranges between 25–70 m were used.

The backscatter data appeared to follow Lambert's rule except where there was a transition from one type of sand to another. The data were blocked into nine groups of ten pings each which, at a scan rate of 1.7° between adjacent pings, would correspond to 17° sectors. The total sector covered was 153°. Within each block, the average Lambert normal incidence backscattering strength 10 log μ was estimated.

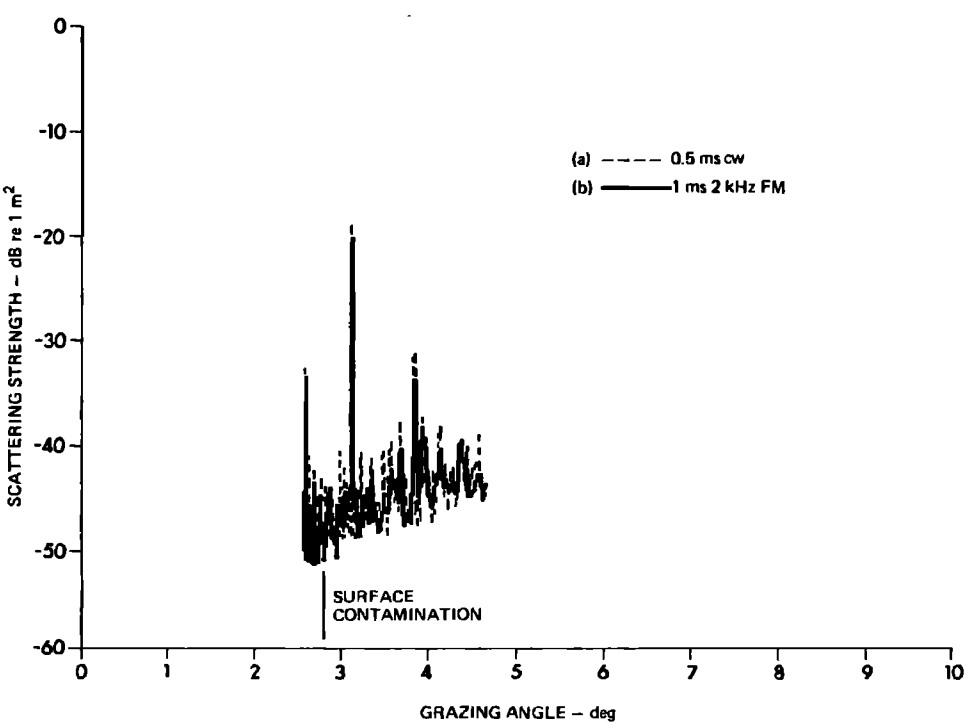

FIG. 17. Comparison of backscattering strength at 80 kHz using (a) 0.5-ms cw and (b) 1-ms, 2-kHz FM pulse types.

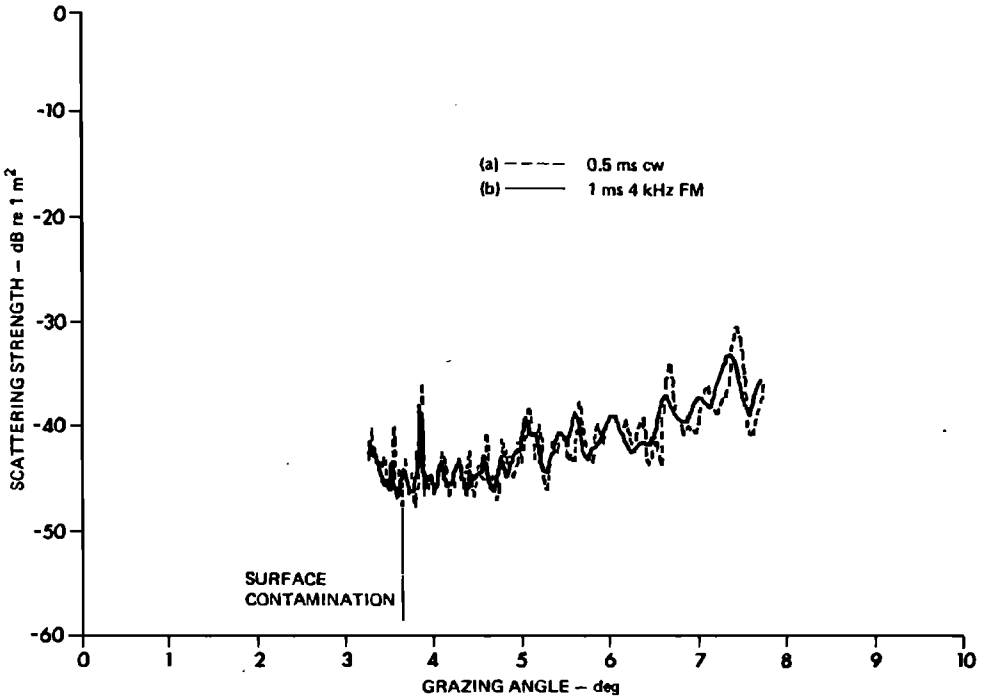

FIG. 18. Comparison of backscattering strength at 95 kHz using (a) 0.5-ms cw and (b) 1-ms, 4-kHz FM pulse types.

Where there was a clear transition from one type of bottom to another, the block was subdivided at the transition range. The results are shown in Fig. 20. The measured values of 10 log μ ranged from -26 to -34 dB; both extreme values were measured over the coarse sand region. At the boundary between the two types of sand, surprisingly, the fine sand showed a higher value of 10 log μ.

Some degree of azimuthal angle dependence is indicated by the analysis results which may be associated with the orientation and structure of sand waves on the bottom. Bottom profile measurements made by NORDA indicate an rms roughness of about 1 cm in the fine sand region and about 2.5–3 cm in the coarse sand region.[10] Divers reported that sand waves in the fine sand region appeared to be randomly oriented and only a few centimeters in lateral extent. The wave heights as well as lateral extent of waves in the coarse sand region were greater.

III. CONCLUSIONS

It was observed that the influence of the sound speed profile was substantial with regard to both the normalization of backscattering strength to unit area and the association of backscattering strength per unit area to grazing angle. In both cases the ray bending at relatively modest ranges was sufficient to produce noticeable differences in levels and grazing angles from those resulting from isovelocity condition assumptions. A more subtle influence upon propagation loss calculations is possible as a result of energy focusing or divergence accompanying sound refraction.

Sound speed profiles were taken about three times a day during the test period and in one location only. This resulted in a rather sparse sampling and undoubtedly contributed to inaccuracies in the data analysis results; however, practical considerations invariably prevent sufficient sampling to characterize the acoustic environment.

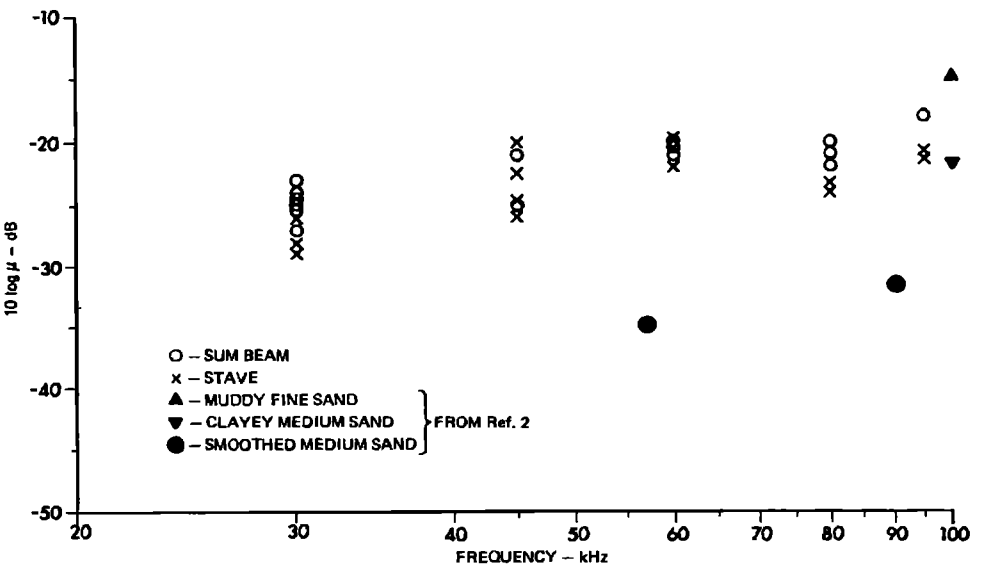

FIG. 19. Estimated values of the bottom backscattering characteristic 10 log μ versus frequency for the fine sand bottom region near San Diego. In all cases the sonar was pointed in azimuth toward the 15-cm (6 in.)-diam sphere. The data include grazing angles from about 2.5° to about 10°.(See text for details of comparison of authors' results with those of Ref. 2.)

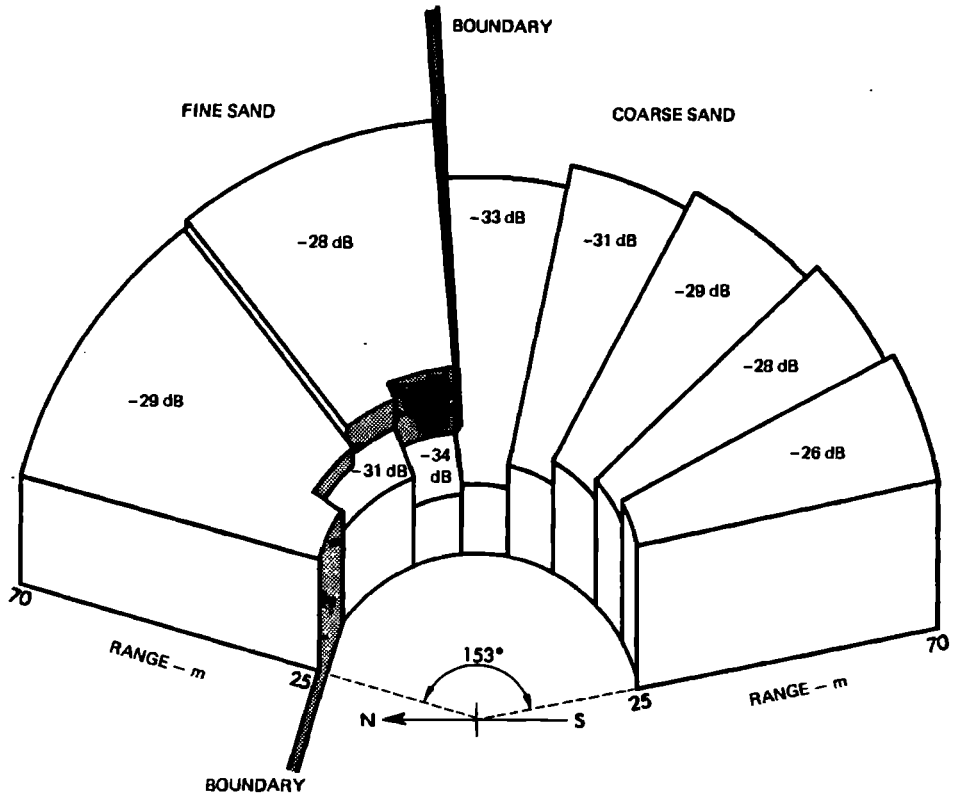

FIG. 20. Measured values of B_0 from a slow azimuthal scan of the bottom. Groups of ten pings, which span sectors of 17°, were blocked and averaged. The measurements were made at 30 kHz with a system beamwidth of 2.8°. The scanned area covered both fine and coarse sand regions, with mean grain sizes 9×10^{-5} m and 5×10^{-4} m, respectively.

The lack of an independent measure of propagation loss is believed to have contributed to the scatter of the data at each frequency. Although fluid-filled spherical acoustic targets were calibrated under free-field conditions and deployed in the bottom measurement region, the deployment geometry, environment, and system parameters combined to prevent the use of this information to help reduce uncertainties in propagation loss. The acoustic targets were very useful as reference points in range and bearing during data acquisition and again during data analyses efforts.

The estimated bottom backscattering strength versus grazing angle plots were often observed to increase with decreasing grazing angle below about 3° as has been reported.[2] The observed background levels at the lower grazing angles were found to depend upon pulse length, to be above ambient noise levels, and to correlate with wind speed. The ranges involved when background levels were observed to increase with decreasing grazing angle were consistent with backscattering from the air–water surface. The spatial and temporal correlations of data from long ranges and low grazing angles were different from similar correlations at shorter ranges and higher grazing angles. The authors feel that the observed behavior at low grazing angles is a result of energy backscattered from the water surface during these acoustic measurements, and that it is not an anomalous characteristic of bottom backscattering.

The bottom backscattering strength was observed to be independent of beamwidth and pulse lengths at all frequencies used in the acoustic measurements.

The frequency dependence of the bottom backscattering strength over the range of frequencies used was observed to follow a 10 $\log f^n$, where n was between 1 and 1.5. This observed behavior is consistent with results reported in Ref. 2.

An azimuthal dependence was observed in the bottom backscattering strength. The acoustic measurement equipment was located near a transition region between fine and coarse sand; data were taken in both regions as the sonar was scanned in azimuth. The highest variability in backscattering strength was observed in the coarse sand region where divers reported larger sand waves than in the fine sand region. Analyses results on bottom roughness are limited at this time; however, the bottom backscattering results observed are expected to be attributable to sand waves and, particularly, to their orientation.

ACKNOWLEDGMENTS

The work was supported by NAVSEA, Code 63R, and NORDA, Code 113. The authors also wish to acknowledge the support of NOSC for the use of the oceanographic tower during the acoustic measurements. We wish also to acknowledge the consultation provided by Dr. John M. Huckabay, Dr. C. Robert Culbertson, and Garland R. Barnard during all phases of this work, and the efforts provided by Paula Taylor and Delores Higdon in the preparation of the manuscript.

[1]T. G. Goldsberry, S. P. Pitt, and R. A. Lamb, "Acoustic Backscatter from the Ocean Bottom," presented at The Acoustical Society of America Meeting, Orlando, Florida, 9–12 November 1982. [Copies of this paper are available from ARL:UT and may be obtained by requesting document number ARL-TP-82-46.]

[2]C. M. McKinney and C. D. Anderson, "Measurements of Backscattering of Sound from the Ocean Bottom," J. Acoust. Soc. Am. 36, 158–163 (1964).

[3]T. J. Schultz, "Undersea Reverberation (U)," Bolt Beranek and Newman, Rep. 4081255 (December 1965), confidential.

[4]A. V. Bunchuk and Y. Y. Zhitkovskii, "Sound Scattering by the Ocean Bottom in Shallow-Water Regions (Review)," Sov. Phys. Acoust. 26, 363–370 (1980).
[5]M. D. Richardson, D. K. Young, and R. I. Ray, "Environmental Support for High Frequency Acoustic Measurements at NOSC Oceanographic Tower, 26 April–7 May 1982; Part I: Sediment Geoacoustic Properties," NORDA Tech. Note 219, Naval Ocean Research and Development Activity, NSTL Station, Mississippi (June 1983).
[6]H. Schulkin and H. W. Marsh, "Sound Absorption in Seawater," J. Acoust. Soc. Am. 34, 864–865 (1962).
[7]R. J. Urick, *Principles of Underwater Sound* (McGraw-Hill, New York, 1975).
[8]H.-K. Wong and W. D. Chesterman, "Bottom Backscattering Near Grazing Incidence in Shallow Water," J. Acoust. Soc. Am. 44, 1713–1718 (1968).
[9]J. J. Crisp, Y. Igarashi, and D. R. Jackson, "First Annual Report on TTCP Bottom Scattering Measurements," The Technical Cooperation Program, Subgroup G (June 1980).
[10]M. D. Richardson, Naval Ocean Research and Development Activity (private communication).